Korean J. Chem. Eng., **26**(6), 1613-1619 (2009)
DOI: 10.2478/s11814-009-0248-x

Gaseous ozone decomposition using a nonthermal plasma reactor with adsorbent and dielectric pellets

Young Sun Mok*,†, Dong Jun Koh, Dong Nam Shin**, and Kyong Tae Kim****

*Department of Chemical & Biological Engineering, Jeju National University, Jeju 690-756, Korea
**Environmental and Energy Research Division, Research Institute of Industrial Science and Technology, Pohang 790-600, Korea
(*Received 30 July 2008 • accepted 31 March 2009*)

Abstract−For the treatment of gaseous ozone emission, this study investigated the adsorption and enrichment of ozone and the destruction of the adsorbed ozone by nonthermal plasma. A nonthermal plasma reactor with adsorbent pellets in it was operated in two sequential modes, adsorption and decomposition of ozone. First, the ozone-containing gas was flowed through the reactor for a given period, in which the ozone was adsorbed and concentrated. In the next step, the gas was switched to argon or nitrogen, bypassing the ozone-containing gas, and AC high voltage was applied to the reactor to produce nonthermal plasma for the decomposition of the adsorbed ozone. By this method, the gaseous ozone was effectively treated with reasonable electrical energy consumption. The adsorbed ozone was converted into molecular oxygen when argon was used as the ozone decomposition gas, whereas a small amount of nitrogen oxides was formed with nitrogen. The energy consumed to decompose the adsorbed ozone was found to be 540 and 795 kJ/g-O_3 decomposed with argon and nitrogen, respectively.

Key words: Gaseous Ozone, Nonthermal Plasma, Adsorption, Decomposition

INTRODUCTION

Ozone is a strong oxidant that has been used in a wide variety of industrial applications including drinking water or wastewater treatment, soil remediation, odor removal, food processing, disinfection, etc. Owing to its high oxidation potential (2.07 V), ozone can effectively oxidize contaminations such as odors, organic and inorganic compounds, and deactivate microorganisms [1-8]. One essential issue regarding the ozone processes is the emission of unreacted ozone (exhaust ozone) [9]. It is well known that exposure to ozone has direct adverse effects on human health like permanent lung injury and respiratory diseases.

Ozone emitted into the air (gas phase ozone) can be abated by several technologies including thermal decomposition, adsorption and catalytic decomposition [10-13]. While many studies on aqueous phase ozone decomposition have been reported, only a few works on gas phase ozone decomposition are available in the literature. Subrahmanyam et al. [13] investigated the decomposition of ozone over activated carbon fiber fabrics or granules at room temperature. Although fresh activated carbon shows high activity for the decomposition of ozone due to its large specific surface area, regular replacements are needed because the formation of CO and CO_2 by the reaction of ozone with carbon and the presence of water vapor to occupy the active sites sharply decrease the activity [13,14]. Thermal decomposition of ozone has a long history [15]. The half-life of ozone largely depends on reaction temperature, and it should be noted that high temperature above 300 °C is required to thermally destroy ozone with reasonable contact time of a few seconds. This high temperature leads to increasing the operational cost of thermal decomposition system. The use of catalyst can lower the ozone decomposition temperature and increase the rate of the decomposition reactions. Unlike activated carbons, catalysts are not consumed during the conversion of ozone into molecular oxygen, assuring long lifetime. It has been reported that various materials such as manganese oxide, alumina, copper oxide, titanium oxide and iron oxide are catalytically active for the decomposition ozone. According to Hao et al. [9], the known catalysts have insufficient activity and stability when they are used under severe conditions such as high ozone concentration, large space velocity and in the presence of moisture.

In this study, the decomposition of exhaust ozone by using nonthermal plasma technology combined with adsorption was investigated. A dielectric-packed bed plasma reactor filled with adsorbent and dielectric pellets in consecutive order was employed. The ozone decomposition process of this study consisted of two steps: adsorption of ozone by passing the exhaust gas through the reactor, followed by nonthermal plasma decomposition in the presence of an inert gas. The dielectric material and the adsorbent filled in the reactor were glass beads and silica gel pellets. In the second step, some adsorbed ozone may desorb to move back to the gas phase, which is destroyed in the reactor section filled with glass beads. The performance of the ozone decomposition system was evaluated with a simulated exhaust gas made by an ozone generator. The effect of several parameters on the decomposition of ozone was examined, and the results were discussed. The energy consumption for the decomposition of ozone was estimated by measuring the amount of ozone adsorbed and the power consumption of the plasma reactor.

EXPERIMENTAL

Fig. 1 depicts a schematic diagram of the experimental apparatus, which was composed of a nonthermal plasma reactor (a dielectric-

†To whom correspondence should be addressed.
E-mail: smokie@jejunu.ac.kr

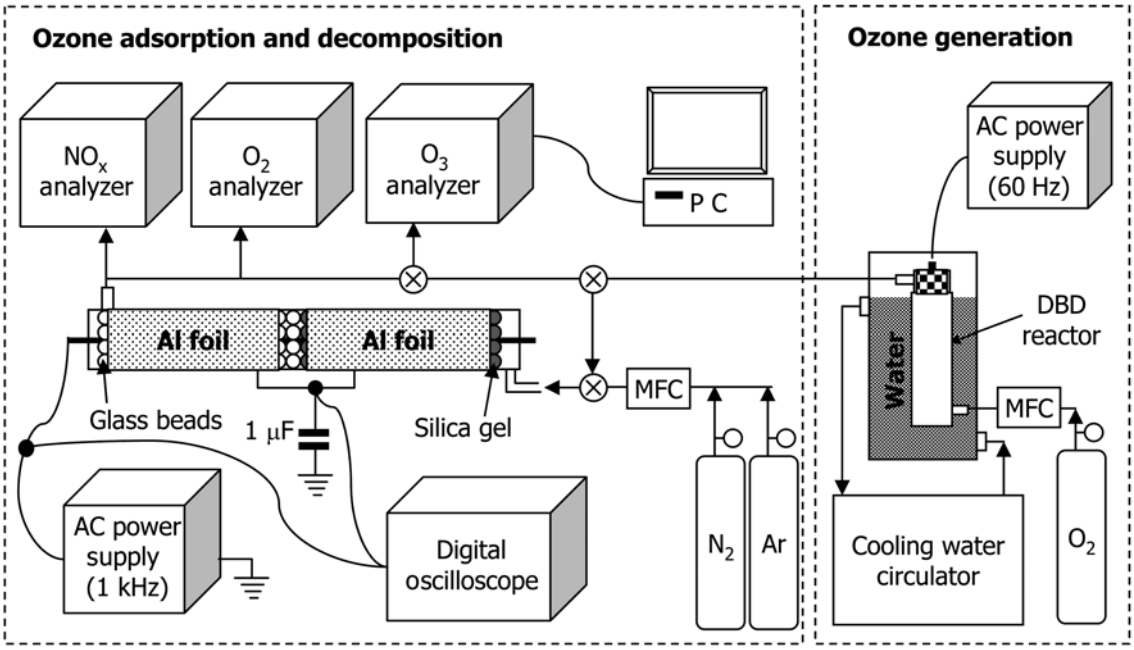

Fig. 1. Schematic diagram of the experimental apparatus.

packed bed reactor), an ozone generator, two AC power supplies for the ozone generator and the nonthermal plasma reactor, a digital oscilloscope, mass flow controllers (MFC), a ultraviolet (UV)-visible spectrophotometer for ozone analysis, an oxygen analyzer, and a NO and NO_2 analyzer.

The dielectric-packed bed reactor, referred to as the plasma reactor was composed of a quartz tube (outer diameter (OD)/inner diameter (ID): 25 mm/22 mm) wrapped with two 100 mm long aluminum foils separated at a certain distance, packing materials (3 mm silica gel pellets, 3 mm glass beads), and a 0.5 mm coaxial nickel-chrome spring wire electrode. The silica gel was purchased from DC Chemical Co. High voltage (AC 1 kHz) was applied to the coaxial electrode acting as the discharging electrode. The aluminum foils were connected to the ground electrode. The discharge region was defined by the length of the aluminum foil. The length of the aluminum foil in the reactor section filled with silica gel pellets as the adsorbent was 100 mm, and that with glass beads was also 100 mm.

The ozone generator, which is a surface discharge reactor, was made up of a quartz tube (OD/ ID: 22 mm/19 mm), a perforated copper tube electrode (OD/ID: 19 mm/18 mm) with holes of 3 mm in diameter, a stainless steel tube electrode (OD/ID: 23 mm/22 mm). The quartz tube, the perforated copper tube and the stainless steel tube were concentrically arranged. The effective length of the ozone generator was 150 mm. The ozone generator was kept at a constant temperature of 20 °C by a cooling water circulator. AC high voltage (operating frequency 60 Hz) was applied to the perforated copper tube electrode while the stainless steel tube electrode was grounded. The flow rate of pure oxygen fed to the ozone generator was 2 L/min.

The gas (mixture of oxygen and ozone) from the ozone generator that was regarded as the simulated exhaust gas was directed to the dielectric-packed bed plasma reactor where ozone adsorption and decomposition occurred. When the gas mixture flowed through the plasma reactor without high voltage applied, the adsorption of ozone took place, thereby being highly concentrated in the adsorbent pellets. After the adsorption step, the ozone-oxygen mixture was closed, and the gas was switched to argon or nitrogen. The argon and nitrogen used were commercial grade. The commercial argon contained oxygen of about 220 ppm as an impurity. In the presence of argon or nitrogen, the application of high voltage to the plasma reactor decomposed the adsorbed ozone to produce molecular oxygen. The flow rate of argon was 1.83 L/min, and that of nitrogen was 2 L/min.

The concentration of ozone was analyzed by a spectrophotometer (Spectro UV-VIS RS, Labomed, Inc.) equipped with a quartz cell (path length: 58 mm) at a wavelength of 260 nm. The concentration of oxygen was analyzed by an oxygen/carbon dioxide analyzer (Model 3600, Illinois Instruments). When nitrogen was used as the ozone decomposition gas, nitrogen oxides were formed, which was analyzed by a chemiluminescent NO-NO_2-NO_x analyzer (Model 42CHL, Thermo Environmental Instruments, Inc.). The voltage applied to the ozone generator and the plasma reactor was measured with a 1,000 : 1 high voltage probe (P6015, Tektronix) and a digital oscilloscope (TDS 3032, Tektronix). The discharge power in the plasma reactor and the ozone generator was estimated by Lissajous charge-voltage figure [16,17]. The power consumed by the nickel-chrome wire electrode was negligible, compared to that for electrical discharge, because the current level was very low. As an example for explaining the discharge power measurement, Fig. 2(a) shows waveforms of the voltage across the electrodes of the plasma reactor and charge deposited on the electrodes, and Fig. 2(b) shows the Lissajous figure that plots the charge versus the voltage. The voltage across the 1 μF capacitor multiplied by its capacitance corresponds to the charge, which is, in principle, equal to the charge deposited on the electrodes of the plasma reactor since the 1 μF ca-

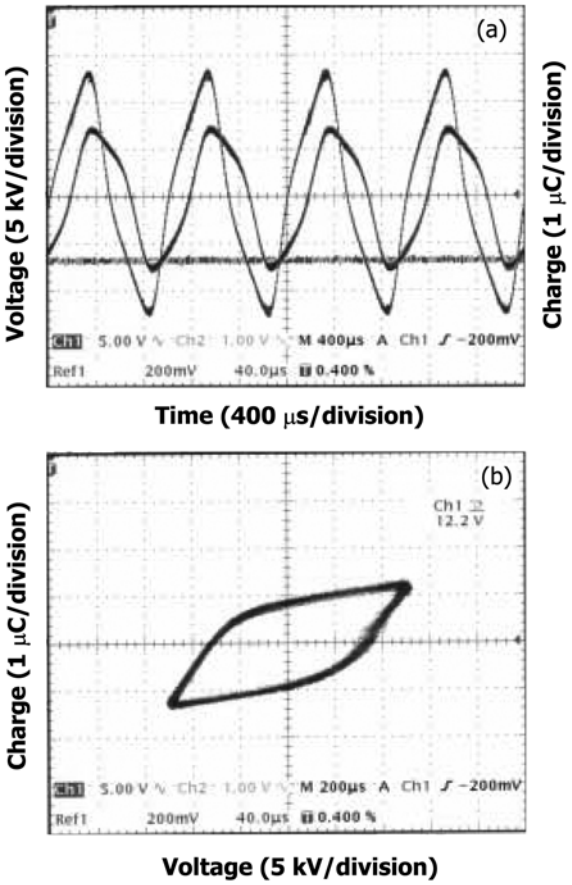

Fig. 2. (a) Waveforms of voltage and charge, (b) Lissajous figure for estimating discharge power (working gas: nitrogen 2.0 L/min).

pacitor and the plasma reactor is a series circuit. The energy per cycle delivered to the plasma reactor is equal to the area of the Lissajous figure, and multiplying the area by the operating frequency gives the discharge power.

RESULTS AND DISCUSSION

1. Ozone Generator

Fig. 3 shows the effect of the applied voltage on the concentration of ozone produced in the ozone generator and the discharge power. The flow rate of oxygen fed to the ozone generator was 2 L/min. When high voltage was applied to the ozone generator, the energetic electrons (e) formed dissociate oxygen molecules by collisions [18]:

$$O_2+e \rightarrow O+O(^1D)+e, \quad k_1=5.0\times10^{-8}\exp(-8.4/T_e) \quad cm^3/s \quad (1)$$

$$O_2+e \rightarrow O+O+e, \quad k_2=4.23\times10^{-9}\exp(-5.56/T_e) \quad cm^3/s \quad (2)$$

Here, T_e is the electron energy in eV. The excited oxygen atom $O(^1D)$ generated by reaction (1) is immediately transformed into O through collisions with oxygen molecules [19]. The oxygen atoms produce ozone as follows [20]:

$$O+O_2+M \rightarrow O_3+M, \quad k_3=8.6\times10^{-31}\,T^{-1.25} \quad cm^6/s \quad (3)$$

$$O_3+O \rightarrow O_2+O_2, \quad k_4=9.5\times10^{-12}\exp(-2300/T) \quad cm^3/s \quad (4)$$

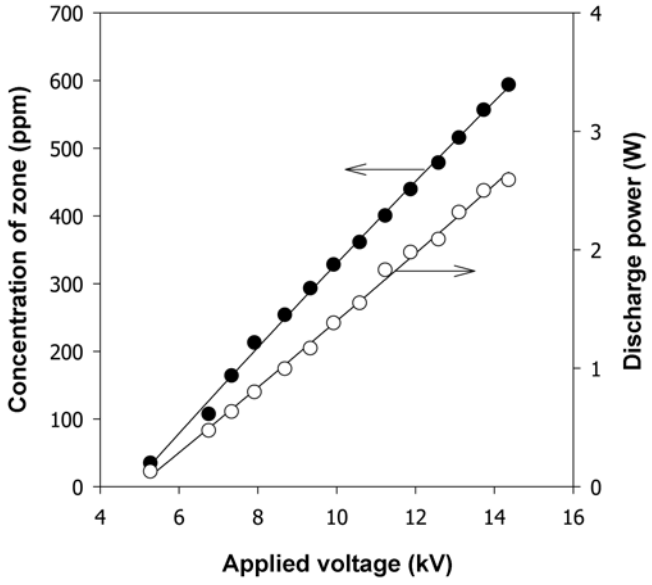

Fig. 3. Concentration of ozone produced in the ozone generator, and discharge power as a function of applied voltage (oxygen flow rate: 2 L/min).

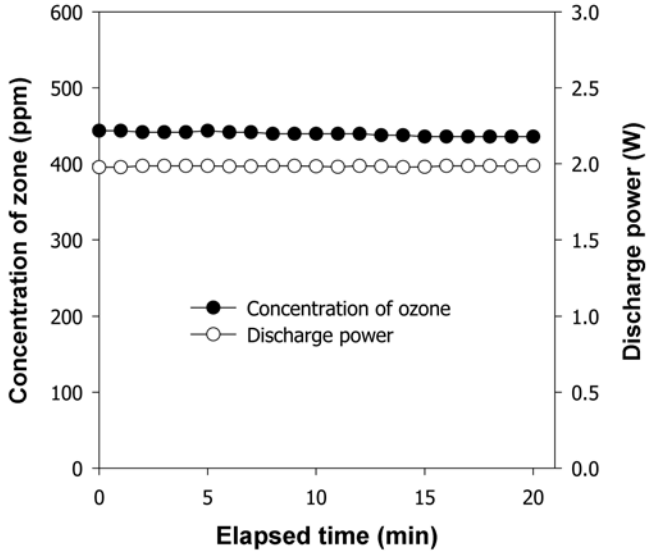

Fig. 4. Variations of ozone concentration and discharge power as a function of elapsed time (oxygen flow rate: 2 L/min).

In reactions (1)-(4), k_1-k_4 are the rate constants of reactions (1)-(4), and M is the third-body reaction partner. The oxygen atom generates ozone by reaction (3), but at the same time, it decomposes ozone by reaction (4). As understood in the rate constants, reaction (3) is favored at lower temperature, whereas reaction (4) at higher temperature. In addition, from the exponent in the rate constant, it is understood that the temperature dependence of reaction (4) is greater than that of reaction (3), i.e., the decomposition reaction gets predominant as the temperature increases. Thus, without cooling the ozone generator, its temperature gradually increases according to the operation time, which is why the ozone generator was kept at a constant temperature. As in Fig. 3, the change in the applied volt-

age from 5.3 to 14.4 kV almost linearly increased the discharge power in the range of 0.13-2.6 W and the concentration of ozone in the range of 35-594 ppm (parts per million, volumetric).

Fig. 4 shows the variations in the discharge power and the concentration of the produced ozone as a function of elapsed time at a voltage of 11.9 kV. As this voltage, the discharge power estimated by the Lissajous figure was 1.98 W and the concentration of ozone was about 440 ppm. As observed, the temporal stability of the ozone generation was good during the operation, because the ozone generator was maintained at a constant temperature, as depicted in Fig. 1. In this study, the ozone-containing gas from the ozone generator was regarded as the simulated exhaust gas, which was directed to the plasma reactor placed downstream. This ozone concentration of 440 ppm is much higher than that emitted in practical ozone processes. For instance, the typical ozone concentration of a cold storage room for treating foods is 2-7 ppm. But, in this study, a high concentration of ozone was used to shorten the experimental time.

2. Plasma Reactor for Ozone Decomposition

The ozone in the simulated exhaust gas was successively treated by adsorption followed by nonthermal plasma decomposition. As described in the experimental section, after the adsorption step, argon or nitrogen was fed to the plasma reactor for decomposing the adsorbed ozone. Fig. 5 compares the discharge power as a function of the voltage applied to the plasma reactor in the presence of argon or nitrogen. When argon was used, the discharge power of 10.4-26.4 W was obtained at voltages of 6.5-11.7 kV. On the other hand, the use of nitrogen needed higher voltage to induce electrical discharge, since the discharge onset voltage with nitrogen is higher. In Fig. 2(b), the voltage intersecting the horizontal axis at charge zero corresponds to the discharge onset voltage, which is about 8 kV. From Fig. 5, it can be seen that the dependence of the discharge power on the voltage with nitrogen was very large, indicating that a slight change in the voltage can significantly affect the decomposition of ozone.

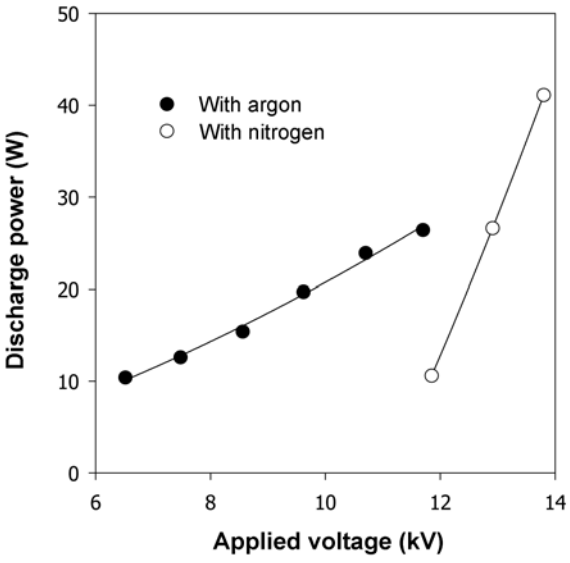

Fig. 5. Discharge power as a function of applied voltage in the presence of argon or nitrogen (argon flow rate: 1.83 L/min, nitrogen flow rate: 2.0 L/min).

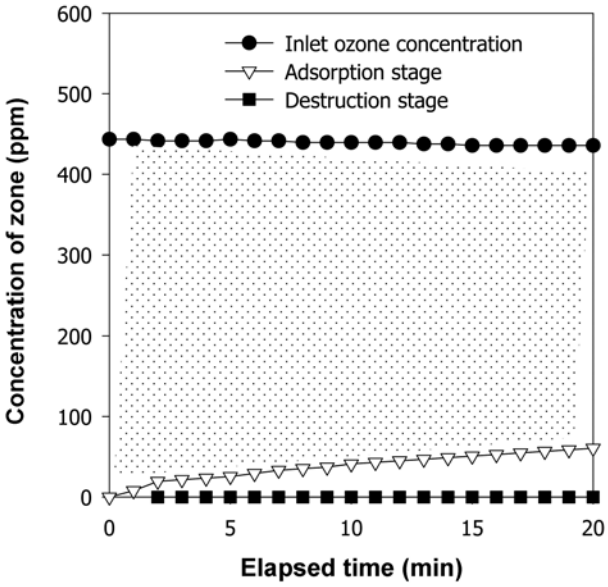

Fig. 6. Concentrations of ozone at the inlet and outlet of the plasma reactor during the adsorption step, and at the outlet during the decomposition step (adsorption time: 20 min, working gas: argon 1.83 L/min).

Fig. 6 presents the concentrations of ozone measured at the inlet and outlet of the plasma reactor during the adsorption step, and at the outlet during the decomposition step. The reaction for the adsorption of ozone can be written as follows:

$$O_3+S \rightarrow O_3\text{-}S \quad (5)$$

where S stands for an active site of the adsorbent. The adsorbed ozone can be decomposed by the action of plasma in the presence of argon or nitrogen. When argon is used, the presumed reactions responsible for the decomposition of ozone can be written as follows:

$$e+Ar \rightarrow e+Ar^* \quad (6)$$

$$e+Ar \rightarrow e+e+Ar^+ \quad (7)$$

$$Ar^*+O_3\text{-}S \rightarrow Ar+O_2+O\text{-}S \quad (8)$$

$$O_3\text{-}S \rightarrow O_3+S \quad (9)$$

$$O_3+O\text{-}S \rightarrow O_2+O_2+S \quad (10)$$

$$Ar^*+O_3 \rightarrow Ar+O_2+O \quad (11)$$

$$O+O_3 \rightarrow O_2+O_2 \quad (12)$$

$$O_2\text{-}S \rightarrow O_2+S \quad (13)$$

Here, e indicates an energetic electron, Ar^* is an excited argon molecule, and O-S is an adsorbed oxygen atom. Besides these reactions, many other reactions simultaneously occur. During the adsorption, most of the ozone in the simulated exhaust gas was removed from the gas phase and concentrated in the adsorbent bed. In Fig. 6, the shaded area corresponds to the amount of ozone adsorbed, which was calculated to be 0.032 g (6.67×10^{-4} mol). After the adsorption step, the gas was switched to argon whose flow rate was 1.83 L/min, and the simulated exhaust gas was closed. The voltage applied to the plasma reactor for decomposing the adsorbed ozone was

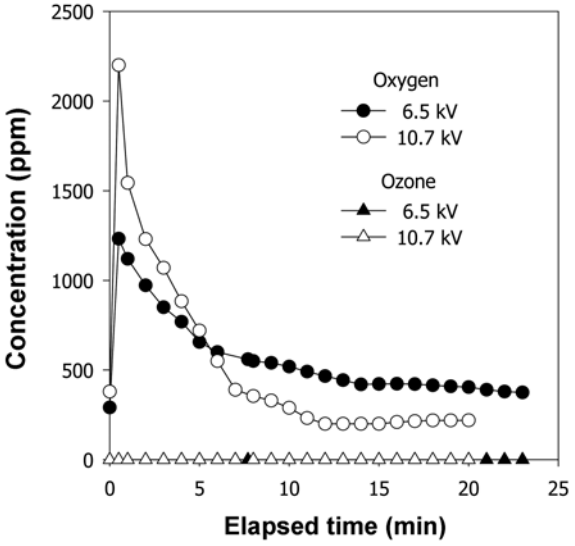

Fig. 7. Variations of oxygen and ozone concentrations at the outlet of the plasma reactor during the decomposition step at different voltages (adsorption time: 20 min, working gas: argon 1.83 L/min).

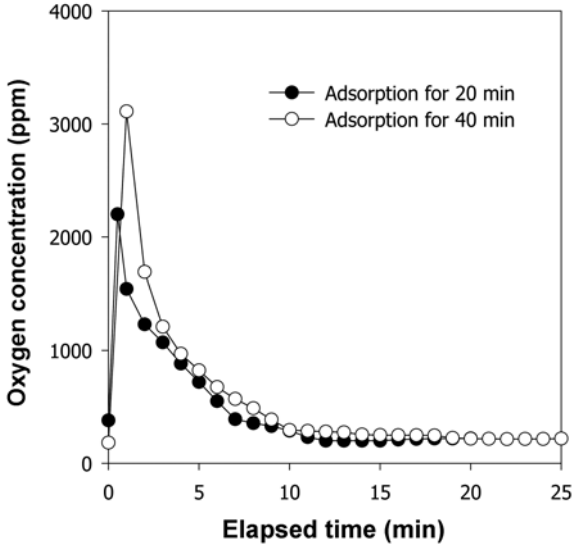

Fig. 8. Variations of oxygen concentration at the outlet of the plasma reactor for different adsorption time (applied voltage: 10.7 kV, working gas: argon 1.83 L/min).

10.7 kV, and at this voltage the discharge power was 24 W. During the decomposition step, ozone was not detected at the outlet of the plasma reactor, indicating that all of the adsorbed ozone was converted into molecular oxygen. The concentration of ozone in the simulated exhaust gas and the adsorption time was 440 ppm and 20 min, respectively. As mentioned above, the concentration of ozone in practical processes is much lower. The adsorption time 20 min at 440 ppm is tantamount to 1,760 min when the concentration of exhaust ozone is 5 ppm. Compared to this practical adsorption time, the decomposition time of 20 min is relatively short.

Fig. 7 shows the variations of oxygen and ozone concentrations at the outlet of the plasma reactor during the decomposition step at different voltages. Argon was used for the decomposition of ozone previously adsorbed in the reactor for 20 min. When the applied voltage was 6.5 kV and 10.7 kV, the discharge power was 10.4 and 24 W, respectively. It should be noted that all of the oxygen measured at the outlet of the plasma reactor was not attributed to the decomposition of ozone. In fact, the silica gel pellets used as the adsorbent can adsorb considerable amount of oxygen as well as ozone. Thus, the concentrations shown in Fig. 7 include the oxygen desorbed from the adsorbent. As observed, at higher voltage, the concentration of oxygen at early stage was higher, and after that, decreased more rapidly, implying that the ozone and oxygen adsorbed in the plasma reactor were removed more quickly. Although the concentration of oxygen at the outlet of the plasma reactor did not decrease to zero due to the impurity oxygen in argon, it did not change from about 12 min, which indicates that the decomposition of the adsorbed ozone was completed in this time. On the other hand, in case of 6.5 kV, the concentration of oxygen was still on the decrease, obviously because the amount of reactive species formed at this voltage was not sufficient to decompose all of the adsorbed ozone within this operation time. The energy consumed to decompose the adsorbed ozone can be calculated as follows. In Fig. 6, the ozone adsorbed in the plasma reactor for 20 min was found to be 0.032 g. In Fig. 7, the energy delivered to the plasma reactor at 10.7 kV is calculated to be 17,280 J (24 W×12 min×60 sec). As a result, the energy consumption is equal to 540 kJ/g-O_3.

Fig. 8 shows the variations of oxygen concentration measured at the outlet of the plasma reactor after the decomposition began, when the adsorption time was different (20 min or 40 min). In both cases, the applied voltage was fixed at 10.7 kV. As in Fig. 8, the concentration of oxygen increased more sharply at the early stage when the adsorption time was 40 min. This is because more ozone and oxygen were adsorbed in the adsorbent bed during the adsorption step, resulting in more oxygen released to the gas phase during the decomposition step. The decomposition of ozone was completed in about 12 min in both cases, indicating that longer adsorption time is favorable in terms of the energy consumption.

As well as argon, other gases such as nitrogen and helium can also be used for the decomposition of the adsorbed ozone. When nitrogen is used, the adsorbed ozone can be decomposed by either excited nitrogen molecules or nitrogen atoms produced by the nonthermal plasma. The reactions related to the decomposition of ozone are as follows:

$$e+N_2 \rightarrow e+N+N \quad (14)$$

$$e+N_2 \rightarrow e+N_2^* \quad (15)$$

$$N_2^*+O_3\text{-}S \rightarrow N_2+O_2+O\text{-}S \quad (16)$$

$$N_2^*+O_3\text{-}S \rightarrow NO+N+O_2+S \quad (17)$$

$$N+O_3\text{-}S \rightarrow NO+O_2+S \quad (18)$$

$$NO+O_3\text{-}S \rightarrow NO_2+O_2+S \quad (19)$$

$$N_2^*+O\text{-}S \rightarrow NO+N+S \quad (20)$$

$$N+O\text{-}S \rightarrow NO+S \quad (21)$$

$$N+NO \rightarrow N_2+O \quad (22)$$

$$N+O_2 \rightarrow NO+O \quad (23)$$

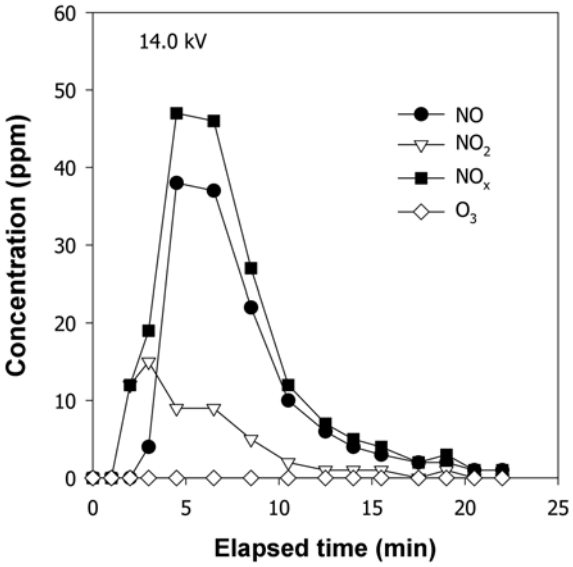

Fig. 9. Concentrations of ozone, NO, NO_2 and NO_x at the outlet of the plasma reactor during the decomposition step (adsorption time: 20 min, working gas: nitrogen 2.0 L/min, applied voltage: 14.0 kV).

where N_2^* stand for an excited nitrogen molecule. As understood in the reactions above, the use of nitrogen not only decomposes the adsorbed ozone, but also forms nitrogen oxides such as NO and NO_2. Once the decomposition of ozone is completed, the formation of nitrogen oxides does not occur. Fig. 9 shows the concentrations of ozone, NO, NO_2 and NO_x (NO plus NO_2) at the outlet of the plasma reactor, which was obtained with nitrogen of 2 L/min and at an applied voltage of 14 kV. As observed, the emission of ozone was not detected at the outlet of the plasma reactor. But, during the decomposition step, nitrogen oxides were formed, mostly in NO. The NO_x level (NO plus NO_2) increased to 47 ppm, and afterward it decreased rapidly. The emission of nitrogen oxides can be a measure to judge whether the decomposition was completed or not. At this experimental condition, it took about 20 min to finish the decomposition of the adsorbed ozone.

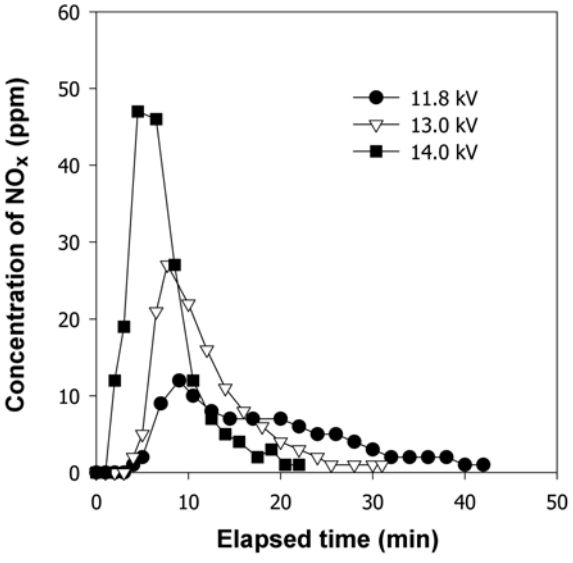

Fig. 10. Effect of the applied voltage on the concentrations of nitrogen oxides emitted during the decomposition step (adsorption time: 20 min, working gas: nitrogen 2.0 L/min).

Fig. 10 presents the effect of the applied voltage on the concentrations of nitrogen oxides emitted during the decomposition step. At voltages of 11.8, 13 and 14 kV, the discharge power was 10.6, 26.6, 41.1 W, respectively. As expected, the higher the voltage was, the more nitrogen oxides were formed, because reactions (14)-(23) were facilitated. But at higher voltage, shorter time was required to complete the decomposition of the adsorbed ozone. The time required to decompose the adsorbed ozone at 11.8, 13 and 14 kV was 20, 25 and 40 min, respectively. Based on these decomposition times, the energy consumption can be calculated at each voltage. As mentioned above, the amount of ozone adsorbed for 20 min was 0.032 g, and the electrical energies delivered to the plasma reactor for 20, 25 and 40 min at voltages of 11.8, 13 and 14 kV were 25,440, 39,900, 49,320 J, respectively. Thus, the energy consumed for the decomposition of 0.032 g ozone is calculated to be 795, 1,246, 1,541 kJ/g-O_3 at voltages of 11.8, 13 and 14 kV. With respect to the energy consumption, lower voltage is desirable, but the decomposition time should also be considered in determining the operating condition. The optimal voltage and decomposition time can be found considering the process economics. Meanwhile, the energy consumption with argon was less than that with nitrogen, as calculated above. But, nitrogen can still be a good candidate since it is cheaper than argon and produces only a small amount of nitrogen oxides.

CONCLUSIONS

A new method proposed in this study, the nonthermal plasma reactor system with adsorbent and dielectric pellets, was found to be very effective for the treatment of gaseous ozone. The treatment process consisted of two steps, the adsorption of ozone and the decomposition of the adsorbed ozone by the nonthermal plasma. When argon was used as the ozone decomposition gas in the second step, all of the adsorbed ozone was converted into molecular oxygen with the energy consumption of 540 kJ/g-O_3 decomposed. On the other hand, the use of nitrogen in the second step produced a small amount of nitrogen oxides. The energy consumption with nitrogen was more than that with argon, depending on the operating condition. But, nitrogen is thought to be a good candidate since it is cheaper than argon. Throughout this study, silica gel was used as the adsorbent packed in the plasma reactor, but further enhancement of this process can be achieved by using other powerful adsorbents such as activated alumina and zeolite.

ACKNOWLEDGMENT

This work was supported by a grant from the KCTV Research Fund of Cheju National University (2008).

REFERENCES

1. A. Demirev and V. Nenov, *Ozone: Sci. Eng.*, **27**, 475 (2005).
2. J. W. Choi, H. K. Song, W. Lee, K.-K. Koo, C. Han and B.-K. Na,

Korean J. Chem. Eng., **21**, 398 (2004).
3. T. Oda, T. Takahashi and K. Yamaji, *IEEE Trans. Ind. Appl.*, **40**, 1249 (2004).
4. S. H. Kong, C. I. Kwon and M. H. Kim, *Korean J. Chem. Eng.*, **20**, 293 (2003).
5. E. J. Rosenfeldt, K. G. Linden, S. Canonica and U. von Gunten, *Water Res*., **40**, 3695 (2006).
6. Y. Sun, Y. Qiu, A. Nie and X. Wang, *IEEE Trans. Plasma Sci.*, **35**, 1496 (2007).
7. S. J. Yoa, Y. S. Cho and J. H. Kim, *Korean J. Chem. Eng.*, **22**, 364 (2005).
8. G.-B. Zhao, S. V. B. J. Garikipati, X. Hu, M. D. Argyle and M. Radosz, *AIChE J.*, **51**, 1800 (2005).
9. Z. Hao, D. Cheng, Y. Guo and Y. Liang, *Appl. Catal. B: Environ.*, **33**, 217 (2001).
10. B. Dhandapani and S. T. Oyama, *Appl. Catal. B: Environ.*, **11**, 129 (1997).
11. R. Radhakrishnan and S. T. Oyama, *J. Catal.*, **199,** 282 (2001).
12. R. C. Sullivan, T. Thornberry and J. P. D. Abbatt, *Atmos. Chem. Phys.*, **4**, 1301 (2004).
13. C. Subrahmanyam, D. A. Bulushev and L. Kiwi-Minsker, *Appl. Catal. B: Environ.*, **61**, 98 (2005).
14. Y. C. Lin, C. L. Chang, T. S. Lin, H. Bai, M. Yan, F. Ko, C. Wu and C. Huang, *Korean J. Chem. Eng.*, **25**, 446 (2008).
15. O. R. Wulf and R. C. Tolman, The thermal decomposition of ozone, in *Proc. Natl. Acad. Sci. USA*, **13**, 272 (1927).
16. U. Kogelschatz, *Plasma Chem. Plasma Proc.*, **23**, 1 (2003).
17. L. A. Rosocha, *IEEE Trans. Plasma Sci.*, **33**, 129 (2005).
18. C. Lee, D. B. Graves, M. A. Lieberman and D. W. Hess, *J. Electrochem. Soc.*, **141**, 1546 (1994).
19. J. Kitayama and M. Kuzumoto, *J. Phys. D: Appl. Phys.*, **30**, 2453 (1997).
20. I. Stefanoviæ, N. K. Bibinov, A. A. Deryugin, I. P. Vinogradov, A. P. Napartovich and K. Wiesemann, *Plasma Sources Sci. Technol.*, **10**, 406 (2001).